Earthquake Engineering & Structural Dynamics
The Journal of the International Association for Earthquake Engineering

EARTHQUAKE ENGINEERING & STRUCTURAL DYNAMICS
Earthquake Engng Struct. Dyn. 2015; **44**:1765–1782
Published online 29 January 2015 in Wiley Online Library (wileyonlinelibrary.com). DOI: 10.1002/eqe.2554

Inelastic spectra to predict period elongation of structures under earthquake loading

E. I. Katsanos[1,2] and A. G. Sextos[1,*,†]

[1]*Department of Civil Engineering, Aristotle University of Thessaloniki, 54124, Thessaloniki, Greece*
[2]*Department of Civil Engineering, Technical University of Denmark, Kongens Lyngby, 2800, Denmark*

SUMMARY

Period lengthening, exhibited by structures when subjected to strong ground motions, constitutes an implicit proxy of structural inelasticity and associated damage. However, the reliable prediction of the inelastic period is tedious and a multi-parametric task, which is related to both epistemic and aleatory uncertainty. Along these lines, the objective of this paper is to investigate and quantify the elongated fundamental period of reinforced concrete structures using inelastic response spectra defined on the basis of the period shift ratio (T_{in}/T_{el}). Nonlinear oscillators of varying yield strength (expressed by the force reduction factor, R_y), post-yield stiffness (a_y) and hysteretic laws are examined for a large number of strong motions. Constant-strength, inelastic spectra in terms of T_{in}/T_{el} are calculated to assess the extent of period elongation for various levels of structural inelasticity. Moreover, the influence that structural characteristics (R_y, a_y and degrading level) and strong-motion parameters (epicentral distance, frequency content and duration) exert on period lengthening are studied. Determined by regression analyses of the data obtained, simplified equations are proposed for period lengthening as a function of R_y and T_{el}. These equations may be used in the framework of the earthquake record selection and scaling. Copyright © 2015 John Wiley & Sons, Ltd.

Received 11 April 2014; Revised 12 November 2014; Accepted 27 December 2014

KEY WORDS: period elongation; inelastic spectra; nonlinear response history analyses; earthquake strong ground motions; force reduction factor

1. INTRODUCTION

During the earthquake strong ground motion excitation, the stiffness and strength of structural systems as well as their ability to dissipate seismic energy degrades with the number of load reversals. This overall softening that structures exhibit after the first inelastic deformation leads them to vibrate with gradually lower apparent, instantaneous natural frequency [1]. The associated elongated fundamental period, being an implicit indicator of seismic damage, is a key issue for the accurate evaluation of structural performance into the nonlinear regime, and as such, it has long attracted scientific attention [2]. Indeed, close correlation has been recognized between the earthquake-imposed structural damage and the modification of the dynamic characteristics (i.e., vibration modes and natural frequencies periods) of structures (e.g., [3]). Several researchers [4–8] have also introduced damage models based on period elongation primarily to evaluate damage of reinforced concrete (R/C) structures. Other studies [9–11] have proposed advanced ground motion intensity measures that account for period lengthening as a means to establish better correlation between strong ground motion characteristics and nonlinear structural response.

The fundamental period of structures and its elongation encountered due to the seismic excitation are also involved in the ground motion selection and scaling procedures. According to most of the

*Correspondence to: A. G. Sextos, Department of Civil Engineering, Aristotle University of Thessaloniki, 54124, Greece.
†E-mail: asextos@civil.auth.gr

current state-of-the-art methods (reviewed by Katsanos *et al.* [12]) and the contemporary seismic codes and relevant guidelines [13–15], the spectral matching period range, within which the selected seismic records have to comply with the target spectrum, is defined as a function of the fundamental period, T_1, and its potential elongation. More precisely, spectral matching is imposed within the period range $0.2\,T_1 < T < 1.5\,T_1$ in the USA, while $0.2\,T_1 < T < 2\,T_1$ in Europe. However, recent studies (e.g., [16]) showed that the uncritical use of a wide-enough period range for spectral matching may lead to highly scattered response results, and thus, implicitly undermines the reliability of the predicted seismic demand. Therefore, it is deemed of high importance to quantify, in a rigorous manner, the extent of fundamental period elongation under earthquake excitation.

The measured seismic response of instrumented buildings and bridges (e.g., [17–22]) and the experimental study of period shifting attributed to successive inelastic episodes in full-scale structural models (e.g., [23–27]) have been widely used to investigate the time-variant, elongated vibration period of structures. A limited number of analytical studies [28–30] have been also conducted to quantify the period lengthening. Notwithstanding the progress already made, the vast majority of research outcome is inevitably case-specific, since it refers to limited structural systems and a small ensemble of earthquake ground motions. On the other hand, the amplitude of period elongation still remains a contradictory issue within the earthquake engineering community, primarily because of its inherent multi-parametric nature and the uncertainty involved. In fact, several researchers (e.g., [18, 31]) concluded that the first-mode vibration period of R/C buildings may be strongly elongated during strong ground shaking (up to 100–130%), while low-to-moderate lengthening of the fundamental period (up to 40–80%) has been observed by others (e.g., [32, 33]).

Given the limitations described previously, the objectives of this paper are to:

(a) quantify the fundamental period lengthening for a variety of structural systems with different elastic periods and complex hysteretic rules, while a large ensemble of strong ground motions was utilized;
(b) investigate the influence of various structural and hysteresis characteristics (including the yield strength, post-yield stiffness and the hysteretic degradation), soil conditions as well as several seismological and strong ground motion parameters (i.e., earthquake magnitude, epicentral distance, frequency content and significant duration) on the inelastic period of structures;
(c) define, through multi-polynomial regression analysis, simplified equations for the prediction of elongated period (T_{in}) as a function of the force reduction factor (R_y) and the reference elastic vibration period (T_{el}) of structures. These equations can be used additionally to re-define the spectral matching period range, required for the code-imposed earthquake records selection procedure.

2. INELASTIC RESPONSE SPECTRA IN TERMS OF PERIOD SHIFT RATIO

2.1. Background

Following the pioneer works of Biot [34] and Housner *et al.* [35], several researchers (e.g., [36–43]) proposed spectral methods to assess structural response. In addition, the peak displacement demand of structures has been defined as a function of the elastic deformation with the use of appropriate inelastic response spectra [44–47]. Such a spectrum type enables the calculation of the target displacement that is involved in the proposed performance-based methods to assess the seismic response of structures (e.g., FEMA-356 [48] and FEMA-450 [49].

2.2. Methodology

The study presented herein introduces the use of novel inelastic response spectra defined in terms of the period shift ratio (i.e., inelastic over elastic predominant period, T_{in}/T_{el}). Particularly, several simple degree of freedom (SDOF) systems with elastic periods, T_{el}, from 0.1 s to 2.5 s were subjected to numerous earthquake motions in order to quantify the fundamental period lengthening for a wide range of structures with different dynamic and structural characteristics. The lateral yield strength, F_y, used to model each one of the oscillators, was determined as a percentage of the minimum yield

DOI: 10.1002/eqe

strength, F_0, required for the system to remain elastic during the ground motion (Figure 1, left). Such a decrease in the yield strength was achieved by dividing the elastic strength demand with the force reduction factor, R_y (Eqn (1)), which is also referred to as the strength ratio.

$$R_y = \frac{F_0}{F_y} = \frac{u_0}{u_y} \tag{1}$$

where u_y and u_0 are the yield and the elastic deformation, respectively.

Five discrete values for R_y ($R_y = 2$–6) and four values regarding the post-yield stiffness ($a_y = 0\%$, 1%, 3% and 10%) were considered to generate a representative sample of various levels of inelasticity. The spread plasticity element, provided by the finite element software IDARC 2D [50], was applied to model the SDOF systems using bilinear backbone curves. The adopted fiber model enabled also the efficient capture of the inelastic response while the embedded yield-oriented model, provided by IDARC 2D (Figure 1, right), was used to account for stiffness degradation, strength deterioration, non-symmetric response and pinching effect. However, the deteriorative effect of reinforcing bars buckling, occurred because of the earthquake loading after crushing of bars surrounding concrete [51], was not considered in this study. Concerning the degrading hysteresis model adopted herein, four parameters control the inelastic loading reversals: α, accounting for stiffness degradation, β_1 and β_2 affecting strength deterioration and the slip parameter γ that controls the pinching because of the closing of the cracks and bond slip, which occurs during the reloading phase. Appropriate values were adopted for the degrading parameters, and consequently, two hysteresis degradation levels (mild and severe) were considered to envelop the period shift prediction because of the earthquake ground motion. Particularly, the adopted values for the degrading parameters are the following: (i) stiffness-degrading parameter, $4 \leqslant \alpha \leqslant 15$; (ii) strength-degrading parameters, $0.08 \leqslant \beta_1,\ \beta_2 \leqslant 0.60$; and (iii) slip parameter, $0.05 \leqslant \gamma \leqslant 0.40$. More details about the degrading rules and the associated parameters can be found elsewhere [30, 50]. Moreover, Figure 2 shows the impact of the degradation levels adopted to the moment–curvature relationship

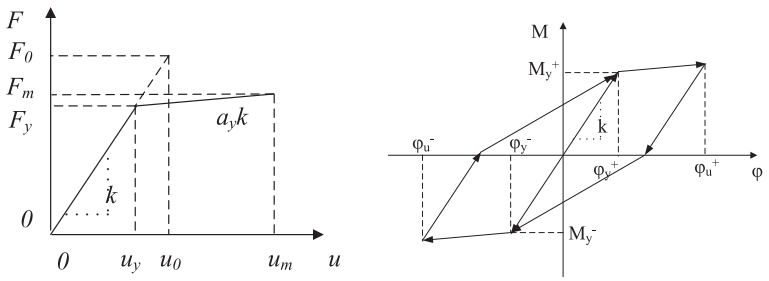

Figure 1. Bilinear force-deformation relationship of the nonlinear system and the corresponding elastic system. F_m and u_m denote the peak force and the maximum deformation of the nonlinear system (left). Yield-oriented law for the cyclic behavior prescribed by IDARC 2D hysteretic model [50] (right).

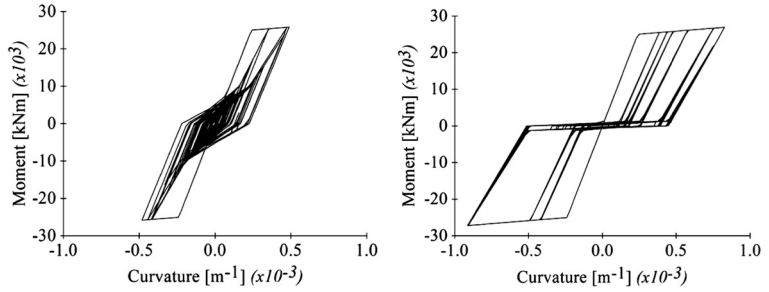

Figure 2. Moment-curvature relationship at the base of the nonlinear oscillator with $T_{el} = 0.7$ s ($R_y = 3$, $a_y = 3\%$) when subjected to the Imperial Valley (Delta, 15.10.1979) earthquake strong motion for the case of a mild (left) and severe (right) degradation rule.

DOI: 10.1002/eqe

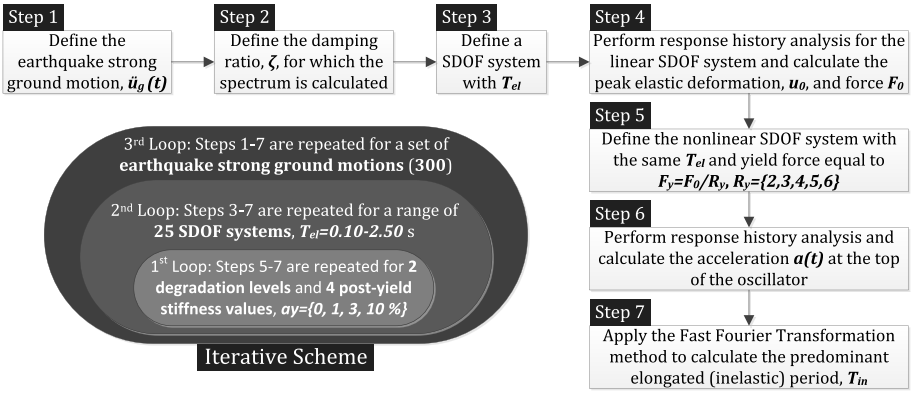

Figure 3. Flowchart of the calculation scheme for the constant-strength inelastic response spectra.

derived at the base of the nonlinear oscillator with elastic period equals to 0.7 s, when subjected to the Imperial Valley (Delta station, 15.10.1979) earthquake strong ground motion. Finally, a low, mass proportional, damping value of 1% was adopted. This equivalent viscous damping represents the non-hysteretic dissipation as the hysteretic damping is already considered. For validation purposes, sensitivity analyses were undertaken until it was verified that further tuning of damping was unnecessary.

Based on Chopra's methodology [52] on constant-strength inelastic response spectra, for each earthquake record and each level of relative strength considered (i.e., five values of force reduction factor, R_y), response history analyses were performed for the set of 25 nonlinear oscillators (period range 0.1 s–2.5 s, time-step of 0.1 s). This computational scheme, presented by Figure 3, also accounts for the variation in post-yield stiffness ($a_y = 0\%$, 1%, 3% and 10%) and the hysteresis degrading levels (mild and severe). In all cases, the predominant inelastic period (T_{in}), required to estimate the period shift ratio (T_{in}/T_{el}), was identified by the algorithm of Fast Fourier Transformation (FFT) applied for the relative acceleration of the oscillator top, with respect to its base acceleration. Hereafter, the inelastic period of a system is defined as the maximum elongated period attained during the entire duration of strong motion ($T_{in} = \max T_{in}(t)$).

3. EARTHQUAKE STRONG GROUND MOTIONS

A rigorous strategy to select an ensemble of appropriate earthquake strong ground motions was developed to reduce the undesirable, inherent uncertainty that is reflected on the structural response [53]. Particularly, a large ensemble of 300 earthquake records (APPENDIX A, Table AI), retrieved by the PEER NGA database [54], was formed including seismic motions with a wealth of different characteristics (Figure 4). Seismological parameters such as the earthquake magnitude, M, the epicentral distance, R (both near-field and far-field motions were adopted), the rupture mechanism and the directivity of seismic waves were considered in selecting the seismic records, while strong ground motions recorded from different soil profiles (i.e., site classes A–E according to National Earthquake Hazards Reduction

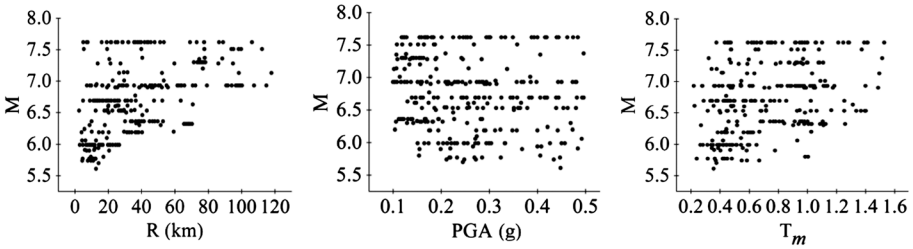

Figure 4. Distribution of the selected strong motions in terms of earthquake magnitude (M), epicentral distance (R), peak ground acceleration (PGA) and mean period (T_m).

DOI: 10.1002/eqe

Program (NEHRP) soil classification [49]) were also used. Moreover, both the frequency content, quantified by the mean period parameter, T_m (introduced by Rathje *et al.* [55]) and the amplitude (peak ground acceleration (PGA)) of strong ground motions were kept deliberately wide. Particularly, different intervals of T_m, indicative of high, moderate and low frequency content, were defined and three mean frequency-based subgroups of 100 strong ground motions (i.e., *F*1, *F*2 and *F*3, Table I) were formed, each one characterized by high spectral amplifications in the short, moderate and long period range, respectively. It is recalled that the mean period parameter, T_m, is derived by weighting the amplitudes over a specified range of the fourier amplitude spectrum:

$$T_m = \frac{\sum C_i^2 \frac{1}{f_i}}{\sum C_i^2} \quad \text{for } 0.25 \text{ Hz} \leqslant f_i \leqslant 20 \text{ Hz with } \Delta f \leqslant 0.05 \text{ Hz} \tag{2}$$

where C_i are the fourier amplitude coefficients, f_i are the discrete FFT frequencies between 0.25 and 20 Hz and Δf is the frequency interval used in the FFT algorithm.

4. ANALYSIS RESULTS

The wide range of parameters involved in the current study led to 300,000 nonlinear response history analyses (corresponding to 300 strong ground motions, 25 elastic vibration periods, five values for the force reduction factor, four values for the post-yield stiffness and two degradation levels), performed with the aid of an in-house software that utilizes the finite element code IDARC 2D [50]. Post-processing and statistical evaluation of the numerical results were implemented using appropriate functions of MATLAB programming language [56], while debugging code was also applied to ensure the reliability of the data produced. For each earthquake record and force reduction factor ($R_y = 2$–6), period shift ratios (T_{in}/T_{el}) were computed. Then, the statistical parameters were obtained regarding the central tendency (i.e., mean value) and the variability of the period shift ratio.

4.1. Central tendency and variability of period shift ratio

Figure 5 (left) shows the constant-strength ($R_y = 2$–6), mean inelastic response spectra in terms of period shift ratio (T_{in}/T_{el}) accounting for the variety adopted in the force reduction factor ($R_y = 2$–6). The inelastic spectra presented herein were calculated for fixed post-yield stiffness ($a_y = 3\%$) and degrading level (mild), allowing to investigate the relation between the degree of inelasticity, indicated by the force

Table I. Uniform distribution of the selected seismic records in terms of the mean period, T_m.

Group	Number of records	Range of T_m (s)	25th percentile of T_m (s)	50th percentile of T_m (s)	75th percentile of T_m (s)
F1	100	0.10 – 0.50	0.30	0.37	0.44
F2	100	0.50 – 0.90	0.58	0.66	0.78
F3	100	0.90 – 1.55	0.99	1.08	1.19

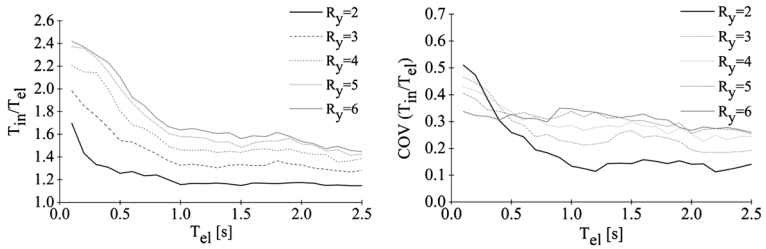

Figure 5. Mean inelastic response spectra in terms of period shift ratio: effect of yield strength level (left). Variability of the period shift ratio (right) ($a_y = 3\%$ and mild degradation level).

DOI: 10.1002/eqe

reduction factor, and the period elongation for the entire set of structural systems examined. As anticipated, higher period elongation (more than 100%, i.e., $T_{in}/T_{el} > 2$) was observed for the weaker structural systems ($R_y = 4$–6), being representative of frame-resisting multistory buildings, irregular structures or structural systems of limited seismic capacity (e.g., designed according to previous code provisions) [28]. The excessive period elongation of *weak systems* was even more pronounced for short period structures ($T_{el} < 0.5$ s), such as poorly designed low-rise buildings. Moreover, the vibration periods of the highly inelastic systems ($R_y = 6$) were elongated, on average, more than 30% compared with the stronger systems ($R_y = 2$), while it can be seen that the mean inelastic spectra in terms of T_{in}/T_{el} present a similar trend, independent on the force reduction factor applied, that is, the stiffer structural systems exhibit higher period elongation for all cases of R_y values. Furthermore, the variability in terms of the T_{in}/T_{el} estimates (expressed by the coefficient of variation, Figure 5 right) was found to increase for the short-period, highly inelastic structural systems ($T_{el} < 0.5$ s). The latter is attributed to the higher scatter of the response results, observed for systems that experience significant inelastic response.

Furthermore, two major spectral regions can be observed in the mean inelastic spectra, as shown in Figure 5 (left). First, for the short-to-moderate stiffness structural systems ($T_{el} < 1.0$ s), the period shift ratio (T_{in}/T_{el}) was found sensitive to T_{el} and decreasing with decreasing stiffness. On the other hand, more flexible structures ($T_{el} > 1.0$ s) present period shift ratio that remains constant with increasing system flexibility. This can be attributed to the fact that yielding of stiff systems drives them to vibration periods statistically associated with higher spectral amplifications (Figure 4), thus inducing consecutive inelastic episodes. On the contrary, the yield of flexible systems leads them to statistically lower spectral accelerations that are not adequate to trigger extensive inelastic response. Overall, the period shift ratios T_{in}/T_{el}, derived for the stiff structural systems ($T_{el} < 0.5$ s), were found, on average, higher by 40% compared with the corresponding ratios of the long period systems ($T_{el} > 1.0$ s).

The same observations, made from Figure 5 (left), are further illustrated in Figure 6 (left), where the elastic vibration periods of the nonlinear oscillators are correlated with the mean values of the inelastic displacement ratio, C_{Ry}. Consistent with notation established by Chopra and Chintanapakdee [44] as well as Ruiz-García and Miranda [57], the C_{Ry} ratio is defined with the following expression:

$$C_{Ry} = \frac{u_m}{u_0} \tag{3}$$

It is noted that both the elastic and inelastic displacement demands (u_0 and u_m) were computed for systems with the same mass and initial stiffness (i.e., common elastic vibration period) when subjected to the same earthquake strong ground motion. Moreover, the subscript R_y denotes systems with known yield strength as defined by the corresponding force reduction factor. Based on Figure 6 (left), the short and moderate period systems ($T_{el} < 1.0$ s) exhibited a pronounced inelastic response (i.e., $C_{Ry} > 2$), which is more profound for the higher values of R_y. On the other hand, the nonlinear oscillators with vibration periods longer than 1.0 s experienced nearly elastic response. In addition, the constant-strength, mean, inelastic spectra in terms of displacement ductility (μ, Figure 6, right), calculated according to Chopra's

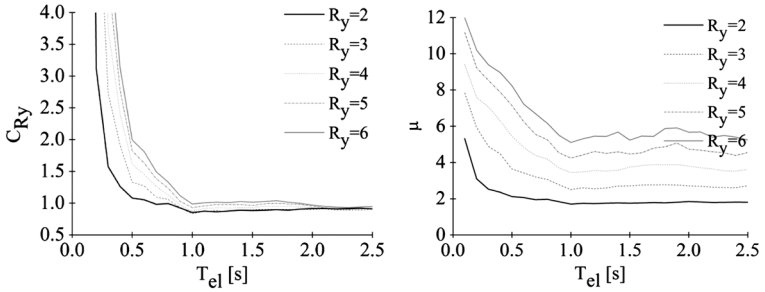

Figure 6. Mean inelastic displacement ratios (left) and mean displacement ductility (right): effect of yield strength level ($a_y = 3\%$ and mild degradation level).

DOI: 10.1002/eqe

methodology [52], emphasized further the severe inelasticity of the short-period systems. It is recalled that the displacement ductility (μ) is defined as follows:

$$\mu = \frac{u_m}{u_y} \tag{4}$$

The trends, shown in Figure 6, among the elastic vibration period (T_{el}), the force reduction factor (R_y) and the inelastic demand (expressed either via C_{Ry} or μ), are also confirmed by relevant studies [44, 57], thus providing further confidence in the specific T_{in}/T_{el} estimates of Figure 5.

4.2. *Effect of post-yield stiffness*

As post-yield stiffness is a critical parameter of the nonlinear constitutional law for the R/C structural members, it was deemed useful to investigate its potential effect on the extent of period elongation under earthquake loading. Figure 7 demonstrates the mean estimates of T_{in}/T_{el}, computed for the 25 vibration periods (oscillators) and the ensemble of 300 seismic motions, accounting for the variation in post-yield stiffness. It is seen that, irrespectively, of the yield strength of structural systems, the post-yield stiffness exerted minor influence on period lengthening over the entire range of natural periods considered ($0.1\,s \leqslant T_{el} \leqslant 2.5\,s$). It is only a mild decrease (approximately 7%) in period elongation that was observed for the nonlinear oscillators modeled with a backbone curve related to the highest post-yield stiffness ($a_y = 10\%$) considered for this study. The significant variation in structural stiffness between the initial branch of the nonlinear constitutional model and the post-elastic branch (Figure 1) governs period shifting. Hence, the additional, but rather marginal, stiffness variation due to different hardening values has a limited impact on T_{in}/T_{el} ratios. The marginal effect of a_y on system's inelasticity was further highlighted by the constant-strength ($R_y = 4$) plot of displacement ductility demand (μ, Figure 8), calculated for each one of the four values of a_y considered. Similar results can be also found elsewhere [44].

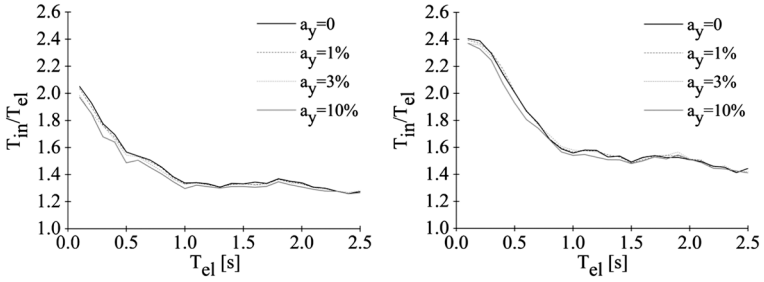

Figure 7. Mean inelastic response spectra in terms of period shift ratio calculated for $R_y = 3$ (left) and $R_y = 5$ (right): effect of post-yield stiffness (mild degradation).

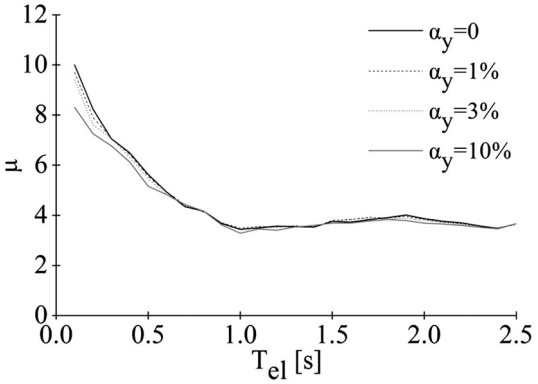

Figure 8. Mean displacement ductility calculated for $R_y = 4$ and mild degradation: effect of post-yield stiffness.

DOI: 10.1002/eqe

4.3. *Effect of hysteretic degradation*

As it was already mentioned, the hysteretic response of the R/C structural members during the earthquake strong ground shaking is seriously affected by stiffness degradation, strength deterioration and pinching effect. In this section, the influence of the previously mentioned three hysteretic deterioration parameters on period lengthening was quantified for two degrading levels, that is, the mild and the severe one. Along these lines, Figure 9 depicts the mean constant-strength ($R_y = \{3,5\}$), inelastic spectra in terms of T_{in}/T_{el} calculated for both the degradation levels considered. Structural systems with severe degradation susceptibility experienced wider period elongation (15–20% on average) compared with their mildly degrading equivalents. The latter, being valid independently on the yield strength of the nonlinear systems, is reasonable mainly for broad-band seismic motions, for which the wealth of the embedded frequencies can induce consecutive nonlinear episodes (and hence higher period elongation) for the constantly degrading structural systems. However, moderately or even severely degrading systems, subjected to narrow-band motions, are possible to experience an early period shift during the first damaging cycles, which may prevent resonance and further inelastic demand. Moreover, Figure 9 shows that the deviation in the fundamental period elongation between the severely and the mildly degrading systems is kept almost constant over the entire range of natural periods considered ($0.1\,\text{s} < T_{el} < 2.5\,\text{s}$). It is interesting to notice that the two characteristic period ranges designated approximately by the threshold value of $T_{el} = 1.0\,\text{s}$, as discussed in Section 4.1, are also evident in Figure 9.

4.4. *Effect of earthquake magnitude and epicentral distance*

To quantify the effect that earthquake magnitude (M) exerts on fundamental period elongation, the ensemble of the selected (300) seismic motions was divided into two magnitude-based subgroups: (i) the $M1$-group including 140 strong ground motions recorded during earthquakes of moderate magnitude, $5.5 \leqslant M \leqslant 6.3$; and (ii) the $M2$-group with 160 seismic motions from more severe earthquake events, $6.3 < M < 8.0$. Similarly, two subgroups of seismic motions were also formed to assess the influence of epicentral distance, R, on the fundamental period lengthening: (i) the $R1$-group with 148 seismic motions recorded at epicentral distances in the range of $2 \leqslant R \leqslant 30\,\text{km}$; and (ii) the $R2$-group that includes 152 far-field earthquake records, $30 < R < 120\,\text{km}$.

Figures 10 and 11 present constant-strength ($R_y = \{3,5\}$), mean inelastic response spectra in terms of T_{in}/T_{el} calculated for the previously mentioned M,R-based subgroups. It was shown that both the earthquake magnitude and the epicentral distance exerted minor influence on the mean estimates of fundamental period lengthening, especially for the nonlinear oscillators of higher yield strength (e.g., $R_y = 3$). Focusing on the effect of earthquake magnitude, it can be observed that, as anticipated, strong ground motions, recorded during severe earthquakes ($M2$-group, $6.3 < M < 8.0$), induced slightly higher fundamental period elongation (6% on average) than the strong motions from moderate seismic events ($M1$-group, $5.5 \leqslant M \leqslant 6.3$). This is more pronounced for the weaker structural systems (e.g., $R_y = 5$, Figure 10, right) and can be possibly attributed to the statistically longer duration of strong ground motions from severe earthquake events (the effect of significant duration on period elongation is thoroughly investigated in the following). In terms of the epicentral distance, it is seen that wider period lengthening (7% on average) is associated with far-field strong motions ($R2$-group, $30 < R < 120\,\text{km}$) in comparison with the near-field ones ($R1$-group, $2 \leqslant R \leqslant 30\,\text{km}$).

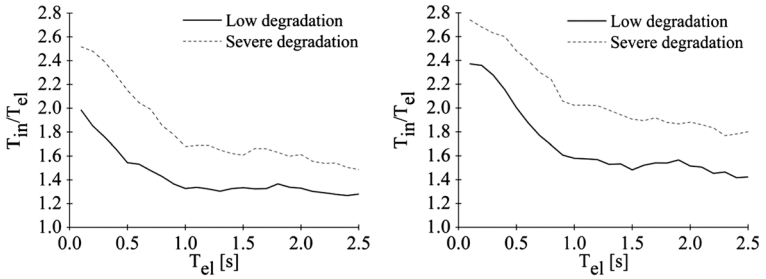

Figure 9. Mean inelastic response spectra in terms of period shift ratio calculated for $R_y = 3$ (left) and $R_y = 5$ (right): effect of hysteretic degradation ($a_y = 3\%$).

DOI: 10.1002/eqe

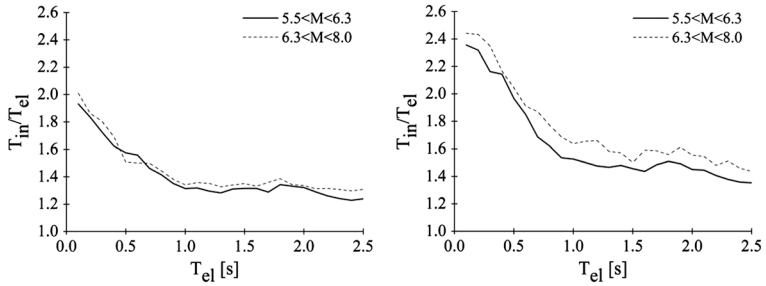

Figure 10. Mean inelastic response spectra in terms of period shift ratio calculated for $R_y = 3$ (left) and $R_y = 5$ (right): effect of earthquake magnitude ($a_y = 3\%$ and mild degradation).

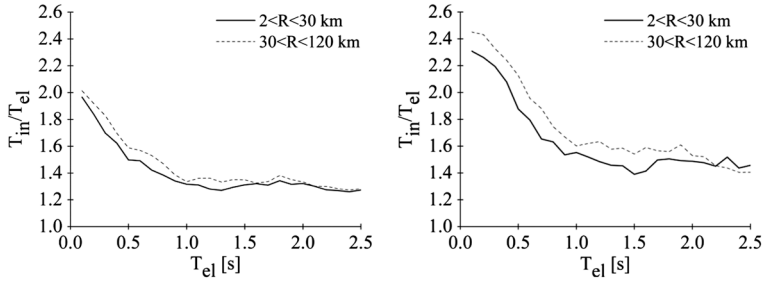

Figure 11. Mean inelastic response spectra in terms of period shift ratio calculated for $R_y = 3$ (left) and $R_y = 5$ (right): effect of epicentral distance ($a_y = 3\%$ and mild degradation).

This trend is mainly observed for the weaker structural systems (e.g., $R_y = 5$, Figure 11, right). It is notable that the short-period systems do not experience higher inelastic period lengthening, although one would expect these systems to be more sensitive to the high frequency content that statistically characterizes a near-field subgroup of motions ($R1$-group, $2 \leqslant R \leqslant 30$ km). It seems that the shorter duration of near-field pulses compensates, to a certain extent, the effect of resonant frequencies.

Several researches (e.g., [44–46, 58–60] have confirmed the minor effect of both the earthquake magnitude and the epicentral distance on several metrics of inelastic demand (i.e., inelastic displacement ratio, displacement-based response indices and complex damage indices) other than the inelastic period lengthening studied herein.

4.5. Effect of soil conditions

Using the initially selected earthquake records (300), two subgroups of seismic motions were created to investigate the influence that soil conditions exert on period lengthening of structural systems. The first subgroup, denoted by $S1$, includes 110 seismic motions recorded on soil profile C according to the NEHRP site classification [49], while the $S2$-group consists of 180 strong motions obtained from soil conditions consistent with site class D. The remaining ten records from the initial set, recorded on A, B and E soil profiles, were deliberately excluded from this soil-related investigation as they did not form an adequate sample to obtain reliable results. Based on NEHRP site classification, the soil categories are defined according to the shear wave velocity ($v_{s,30}$) of the uppermost 30 m of the soil column. Along these lines, $360 \leqslant v_{s,30} \leqslant 760$ m/s and $180 \leqslant v_{s,30} \leqslant 360$ m/s correspond to the site classes C and D, respectively used herein.

Figure 12 plots the constant-strength ($R_y = \{3,5\}$), mean inelastic spectra in terms of the period shift ratio, computed for the 25 natural periods (oscillators) when subjected to both S-groups of earthquake strong ground motions. First, it was found that period elongation was only marginally affected by soil conditions (C and D classes), particularly for the long period systems with $T_{el} \geqslant 1.5$ s. This observation is valid independently of the yield strength of the systems studied (Figure 12). Although the previously mentioned effect of site class was indeed minor, it is noted that strong motions recorded on softer soil profiles lead to a more extensive inelastic response (8% on average). Second, it is critical to note that such a study for the effect of soil conditions on the inelastic demand should also account for the soil

DOI: 10.1002/eqe

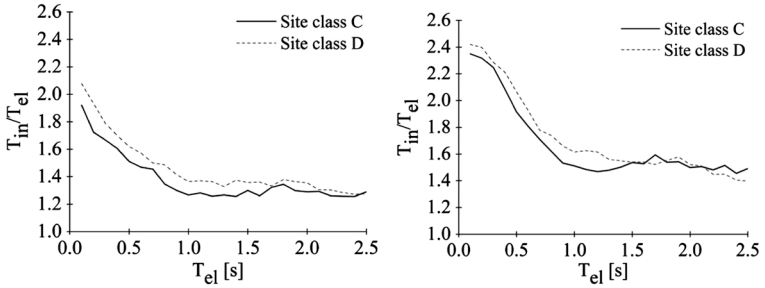

Figure 12. Mean inelastic response spectra in terms of period shift ratio calculated for $R_y = 3$ (left) and $R_y = 5$ (right): effect of soil conditions ($a_y = 3\%$ and mild degradation).

flexibility, because soil-structure interaction (SSI) phenomena can severely modify the structural response under the earthquake excitation. Nevertheless, because of the already wide range of parameters considered herein, SSI effects were excluded from the current investigation.

4.6. Effect of frequency content of strong ground motion

An additional investigation was performed to identify the sensitivity of first-mode period elongation on the frequency content of earthquake excitation. It is recalled that the frequency content was quantified on the basis of the mean period parameter, T_m (Eqn (2)), according to which three subgroups of 100 seismic motions were formed (Chapter 3). Figure 13 illustrates the constant-strength ($R_y = \{3,5\}$), mean inelastic spectra in terms of the mean period shift ratio (T_{in}/T_{el}), computed for the 25 vibration periods and the three *F*-groups of strong ground motions. It was shown that structural systems, excited with strong ground motions of low frequency content (F3 group – $0.90 \leqslant T_m \leqslant 1.55$ s), experienced higher period elongation (20% on average) than the systems subjected to motions with higher frequency content (subgroups *F*1 and *F*2*)*. This observation is valid independently of the systems yield strength ($R_y = \{3,5\}$).

To understand the reasons that low frequency content motions induced higher period elongation compared with the seismic motions of higher frequency content, one may focus on Figure 14, where the elastic response spectra of two characteristic seismic records (Stone Canyon, Northridge – 17.01.1994 and Hollister City Hall, Loma Prieta – 18.10.1989) and their effect on period elongation are plotted. The Northridge record is indicative of low mean period ($T_m = 0.39$ s) in contrast to the Loma Prieta record ($T_m = 1.12$ s). It is observed (Figure 14, right) that systems with T_{el} lower than the mean period of the strong motion experience significant period elongation. Particularly, for the Loma Prieta record, nonlinear systems with $T_{el} < T_m$ exhibit $1.6 < T_{in}/T_{el} < 2.6$ in contrast to the case of Northridge earthquake record, where period shift does not exceed 1.6. This is clearly associated with the observations already made in Section 4.1, which yielding of systems with $T_{el} < T_m$ leads them to amplified spectral accelerations that in turn induce consecutive inelastic episodes. The extreme example is illustrated within the period range 0–0.5 s, where the Loma Prieta earthquake

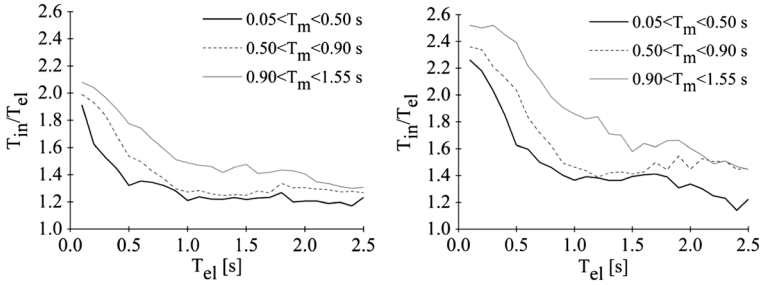

Figure 13. Mean inelastic response spectra in terms of period shift ratio calculated for $R_y = 3$ (left) and $R_y = 5$ (right): effect of strong ground motions frequency content ($a_y = 3\%$ and mild degradation).

DOI: 10.1002/eqe

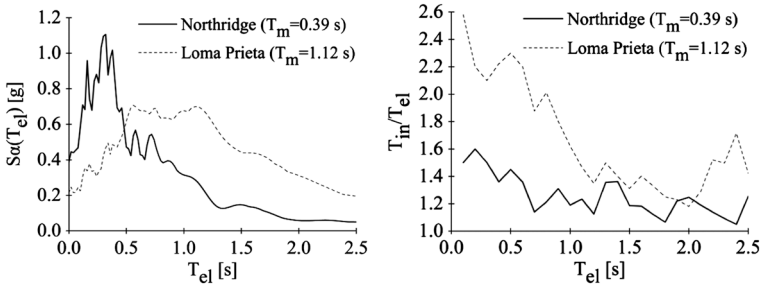

Figure 14. Elastic response spectra (left) and inelastic response spectra in terms of period shift ratio (right, $R_y = 4$–$a_y = 3\%$ – mild degradation), calculated for the Northridge (Stone Canyon, 17.01.1994) and the Loma Prieta (Loma Prieta, 18.10.1989) earthquake strong ground motions.

motion induced almost twice as high period elongation (2.6/1.4 = 1.85) even though its spectral accelerations are almost half than those of the Northridge record.

4.7. *Effect of significant duration of strong ground motion*

A final investigation was made to relate the duration of strong motion with period elongation of inelastic systems. Among the large variety of definitions to identify the earthquake record duration [61], the significant duration, introduced by Trifunac and Brady [62], was adopted herein. It is recalled that the cumulative Arias intensity, $h_{\text{Arias}}(t)$, as expressed by Eqn (5), can be calculated for each earthquake record using the Husid plot that tracks the build-up of seismic energy in time [63]. The parameter of significant duration, SD595, is then determined as the time interval between the low and high 5% cut-offs of the energy accumulated (i.e., 5–95% of the h_{Arias}).

$$h_{\text{Arias}(t)} = \frac{\int_0^t a^2(t)dt}{\int_0^{T_{\text{motion}}} a^2(t)dt} \tag{5}$$

where $\alpha(t)$ and T_{motion} are the acceleration time history and the total duration of the strong ground motions, respectively. The choice for the specific metric of strong motion duration was driven by the well correlation that has been found between the SD595 parameter and the inelastic demand (e.g., [64]).

In order to quantify the influence of strong motion duration on period lengthening of structural systems, the initially selected ensemble of 300 earthquake records was divided into three subgroups ($D1$–$D3$) indicative of short (107 seismic motions with $0 < \text{SD595} \leqslant 10$ s), moderate (113 seismic motions with $10 < SD595 < 18$ s) and long (80 seismic motions, $18 \leqslant \text{SD595} \leqslant 40$ s) significant durations, respectively. Figure 15 plots the constant-strength ($R_y = \{3,5\}$), mean inelastic response spectra in terms T_{in}/T_{el}, computed for the 25 periods and the three D-groups of strong motions. First, the effect of significant duration on period lengthening was found negligible for the case of stronger ($R_y = 3$) and stiffer ($T_{el} \leqslant 0.6$ s) structural systems (Figure 15, left). It is only weaker ($R_y = 5$) and flexible ($T_{el} > 1.0$ s)

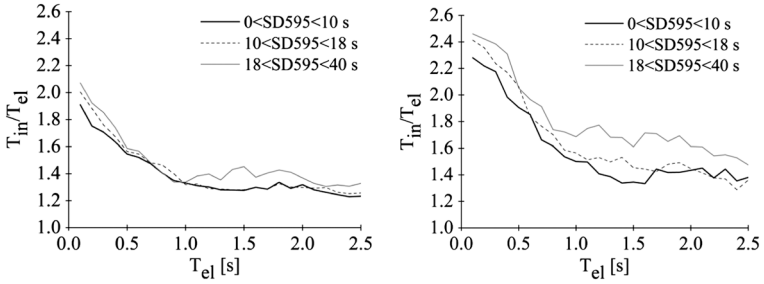

Figure 15. Mean inelastic response spectra in terms of period shift ratio calculated for $R_y = 3$ (left) and $R_y = 5$ (right): effect of the significant duration, SD595, of earthquake strong ground motions ($a_y = 3\%$ and mild degradation).

DOI: 10.1002/eqe

structural systems, where motions with higher duration induced higher inelastic response (Figure 15, right). This observation is consistent with intuition, as long duration motions by definition induce a larger number of inelastic cycles. The correlation of advanced inelastic structural demand with strong motion duration is in agreement with other studies [64–66]. It is, though, notable that the structural systems were subjected herein only to single earthquake motions. Hence, the inelastic response may be further investigated by using multiple earthquake excitations (seismic swarms of mainshock–aftershock sequences [67–70]).

5. SIMPLIFIED EQUATIONS

Based on the research results presented previously, simplified equations were proposed to predict the period shift ratio, T_{in}/T_{el}, as a function of yield strength (R_y) and natural elastic period (T_{el}). The necessity for such a relationship arises from the fact that most code-based records selection and scaling procedures implicitly relate the spectral matching period with the expected extent of first-mode period elongation (T_1). In particular, this spectral range extents up to 1.5 T_1 in the US structural design codes [14] and to 2 T_1 in Eurocode 8 – Part 1 [13], without any clear justification and distinction among different structural systems. Additionally, Eurocode 8 relatively wider spectral matching period range has been recently associated with undesirably high-scattered structural response estimates [16, 71].

Along these lines, polynomial regression analysis was performed using the least-squares technique to derive simplified expressions that more reliably predict the mean period elongation as a function of the elastic period, T_{el}, of structural systems with known lateral strength, quantified by the force reduction factor, R_y. Table II presents the coefficients of the 6th order polynomials (Eqn (6)), calculated from the regression analysis, while Figure 16 plots the mean period shift ratio, predicted by the aforementioned

Table II. Polynomial coefficients to be used in Eq. (6).

Force reduction factor	Coefficients of 6th order polynomial terms							
(R_y)	a_1	a_2	a_3	a_4	a_5	a_6	a_7	R^2 (%)[a]
2	0.288	−2.404	7.839	−12.646	10.624	−4.542	2.037	98.34
3	0.118	−0.838	2.235	−2.954	2.529	−1.894	2.151	99.52
4	−0.141	1.402	−5.325	9.441	−7.397	1.347	2.136	99.18
5	−0.144	1.402	−5.301	9.486	−7.601	1.429	2.303	99.59
6	−0.153	1.511	−5.716	10.205	8.236	1.730	2.306	96.04

[a]The coefficient of determination, denoted R^2, indicates the accuracy of the regression performed. The higher the R^2 ($0 \leqslant R^2 \leqslant 1$), the better prediction can be achieved with the use of the model derived after the regression analysis.

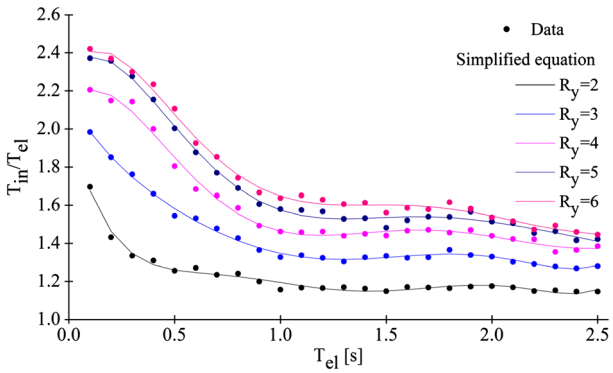

Figure 16. Simplified equations to predict the fundamental period lengthening for structures with different yield strength.

DOI: 10.1002/eqe

equation for each level of yield strength (i.e., force reduction factor, R_y) considered. It can be seen that the proposed functional form provides accurate enough estimates of T_{in}/T_{el}, because it converges to the data-based mean estimations of period elongation. The latter, being verified by the close-to-unity values of R^2 (coefficient of determination, Table II), is the main reason for selecting the particular polynomial functional configuration, among others, for the T_{in}/T_{el} equation.

$$\frac{T_{in}}{T_{el}} = a_1 T_{el}^6 + a_2 T_{el}^5 + a_3 T_{el}^4 + a_4 T_{el}^3 + a_5 T_{el}^2 + a_6 T_{el} + a_7 \tag{6}$$

6. CONCLUSIONS

The study presented herein was conducted to assess the fundamental period elongation that structural systems experience under earthquake loading. Period lengthening, being an implicit indicator of structural inelasticity, was quantified using constant-strength, mean inelastic response spectra calculated in terms of the period shift ratio (T_{in}/T_{el}). Nonlinear oscillators of varying yield strength (expressed by the force reduction factor, R_y), post-yield stiffness (a_y) and advanced hysteretic laws, which account for both stiffness and strength degradation as well as the pinching effect, were examined for a large number (300) of strong motions carefully selected on the basis of a multi-criterion strategy. A total number of 300,000 nonlinear response history analyses were performed to investigate the sensitivity of inelastic period in several ground motion and structural parameters. The main conclusions drawn can be summarized in the following:

(a) Wider period elongation ($T_{in}/T_{el} > 2$) was observed for the weaker structural systems ($R_y = 4$–6) especially in the short period range ($T_{el} < 0.5$ s). A common trend was also observed irrespectively of the yield strength considered: the stiffer the structural systems, the more extensive the period elongation. Moreover, the flexible structures ($T_{el} > 1.0$ s) presented period shift ratios that remained constant with increasing system flexibility. On the other hand, for systems of short-to-moderate stiffness ($T_{el} < 1.0$ s), the period shift ratio was found sensitive to T_{el} and decreasing with decreasing stiffness.

(b) Irrespectively of the yield strength of structural systems, the post-yield stiffness (a_y) was found to exert marginal influence on period lengthening over the entire period range examined (i.e., $0.1\text{ s} \leqslant T_{el} \leqslant 2.5$ s).

(c) Structural systems that experienced severe degradation (i.e., stiffness and strength degradation as well as pinching effect) under the seismic motions exhibited wider period elongation (on average 15–20%) than the mildly degrading systems. This deviation in T_{in}/T_{el} was found almost constant over the entire period range considered.

(d) The earthquake magnitude, the epicentral distance in addition to the soil conditions played only a minor role to the elongated period of the nonlinear oscillators. This observation is valid independently of the force reduction factor (R_y) applied.

(e) Nonlinear structural systems, excited with low frequency content strong motions ($0.90 \leqslant T_m \leqslant 1.55$ s), exhibited higher period elongation (20% on average) than the systems subjected to motions with higher frequency content. This deviation in T_{in}/T_{el} estimates, observed independently of the structures' yield strength, is attributed to the consecutive inelastic episodes that systems with $T_{el} < T_m$ statistically experience.

(f) The effect of ground motion (significant) duration on period lengthening was found negligible for the case of stronger ($R_y = 3$) and stiffer ($T_{el} \leqslant 0.6$ s) structural systems. The duration of strong ground motion had an evident impact on inelastic response only for weaker ($R_y = 5$) and flexible ($T_{el} > 1.0$ s) oscillators.

(g) Polynomial regression analysis of the data derived was performed to calculate closed-form equation to predict period shift ratio (T_{in}/T_{el}) as a function of the force reduction factor, R_y, and the natural vibration period, T_{el}. The reliable estimates of the fundamental inelastic period, obtained with the proposed expressions, can be used to redefine the spectral matching period bandwidth, which is involved into the current code-based records selection and scaling procedures.

DOI: 10.1002/eqe

7. NOTATION

The following symbols are used in this paper.

α	Stiffness degrading parameter of the hysteresis model
β_1, β_2	Strength deterioration parameters of the hysteresis model
γ	Slip parameter of hysteresis model
μ	Displacement ductility
φ_u	Ultimate curvature
φ_y	Yield curvature
$a(t)$	Acceleration time-history
a_y	Post-yield stiffness
$a_1,\ldots, a_7$	Polynomial coefficients used for the regression model
C_i	Fourier amplitude coefficient
C_{Ry}	Inelastic displacement ratio
f_i	Discrete frequency for Fast Fourier Transformation
F_m	Maximum force of the nonlinear system
F_y	Yield force
F_0	Elastic force
h_{Arias}	Arias intensity
M	Earthquake magnitude
M_y	Yield moment
PGA	Peak ground acceleration
R_y	Force reduction factor
SD595	Significant duration
$Sa(T)$	Spectral acceleration specified at period T
T_{el}	Elastic period of SDOF system
T_{in}	Inelastic (predominant) period of SDOF system
T_m	Mean period of strong ground motion
T_{motion}	Total duration of strong ground motion
T_1	Fundamental elastic period of structures
u_m	Maximum deformation of the nonlinear system
u_y	Yield deformation
u_0	Elastic deformation
$v_{s,30}$	Shear-wave velocity at the upper 30 m of soil profile

APPENDIX A

Table AI. Earthquake events used in this study and related information.

Earthquake name (Date)	Magnitude	Distance (km) R_{min}–R_{max}	Records	Site class[a,b]
Kern County (1952.07.21)	7.36	88.39	1	C(1)
Northern California (1954.12.21)	6.50	30.79	1	D(1)
Parkfield (1966.06.28)	6.19	32.56–40.26	3	C(1) + D(2)
Borrego Mountain (1968.04.09)	6.63	70.75	1	D(1)
San Fernando (1971.02.09)	6.61	20.04–39.49	5	C(4) + D(1)
Managua, Nicaragua (1972.12.23)	6.24	5.68	1	D(1)
Friuli, Italy (1976.05.06)	6.50	20.23	1	C(1)
Tabas, Iran (1978.09.16)	7.35	20.63–74.66	2	C(1) + D(1)
Coyote Lake (1979.08.06)	5.74	4.37–10.94	4	C(1) + D(3)
Imperial Valley (1979.10.15)	6.53	2.47–43.15	18	D(18)

(Continues)

DOI: 10.1002/eqe

Table AI. (Continued).

Earthquake name (Date)	Magnitude	Distance (km) R_{min}–R_{max}	Records	Site class[a,b]
Livermore (1980.01.24)	5.80	17.13	1	D(1)
Mammoth Lakes (1980.05.25)	5.94	5.90–14.19	7	D(7)
Victoria, Mexico (1980.06.09)	6.33	36.67	1	D(1)
Trinidad and Tobago (1980.11.08)	7.20	76.75	2	D(2)
Corinth, Greece (1981.02.24)	6.60	19.92	1	D(1)
Westmorland (1981.04.26)	5.90	7.02–20.47	3	D(3)
Coalinga (1983.05.02)	6.36	4.60–52.86	22	C(9) + D(13)
Morgan Hill (1984.04.24)	6.19	3.94–38.20	5	C(2) + D(3)
Taiwan-SMART1-40 (1986.05.20)	6.32	65.48–70.27	8	D(8)
North Palm Springs (1986.07.08)	6.06	4.24–6.28	2	D(2)
Chalfant Valley (1986.07.20)	6.19	10.54–31.25	4	D(4)
San Salvador, El Salvador (1986.10.10)	5.80	9.54	1	D(1)
Taiwan-SMART1-45 (1986.11.14)	7.30	71.35–78.21	15	C(1) + D(14)
New Zealand (1987.03.02)	6.60	24.23	1	C(1)
Whittier Narrows (1987.10.01)	5.99	2.86–26.55	25	C(11) + D(14)
Superstition Hills (1987.11.24)	6.54	19.51–35.83	3	D(3)
Spitak, Armenia (1988.12.07)	6.77	36.19	1	D(1)
Loma Prieta (1989.10.18)	6.93	7.17–114.87	42	B(1) + C(19) + D(17) + E(5)
Manjil, Iran (1990.06.20)	7.37	40.43–77.84	2	C(1) + D(1)
Sierra Madre (1991.06.28)	5.61	12.64	1	C(1)
Erzincan, Turkey (1992.03.13)	6.69	8.97	1	D(1)
Cape Mendocino (1992.04.25)	7.01	22.64–53.34	3	C(1) + D(2)
Landers (1992.06.28)	7.28	13.67–94.77	6	C(2) + D(4)
Big Bear (1992.06.28)	6.46	40.46	1	D(1)
Northridge (1994.01.17)	6.69	4.85–63.53	33	A(1) + B(1) + C(16) + D(15)
Kobe, Japan (1995.01.16)	6.90	19.25–55.81	10	A(1) + D(9)
Northwest China (1997.04.11)	6.10	19.11	1	D(1)
Kocaeli, Turkey (1999.08.17)	7.51	5.31–112.26	9	B(1) + C(1) + D(6) + E(1)
Chi-Chi, Taiwan-1 (1999.09.20)	7.62	4.96–106.20	39	C(31) + D(8)
Chi-Chi, Taiwan-2 (1999.09.20)	6.20	10.10–59.29	3	C(2) + D(1)
Chi-Chi, Taiwan-3 (1999.09.25)	6.30	8.80–51.51	4	C(2) + D(2)
Hector Mine (1999.10.16)	7.13	26.53–117.88	4	C(2) + D(2)
Duzce, Turkey (1999.11.12)	7.14	29.27–31.56	2	C(1) + D(1)

[a]According to the National Earthquake Hazards Reduction Program site classification [49]: site class A ($v_{s,30} \geqslant 1500$ m/s), site class B (760 m/s $< v_{s,30} \leqslant 1500$ m/s), site class C (360 m/s $< v_{s,30} \leqslant 760$ m/s), site class D (180 m/s $< v_{s,30} \leqslant 360$ m/s) and site class E ($v_{s,30} \leqslant 180$).
[b]In the last column, number in the parenthesis indicates the number of records for given site class.

REFERENCES

1. Udwadia FE, Trifunac DM. Time and amplitude dependent response of structures. *Earthquake Engineering and Structural Dynamics* 1974; **2**(4):359–378.
2. Elnashai AS, Di Sarno L. *Fundamentals of Earthquake Engineering*. John Wiley & Sons Ltd: UK, 2008.
3. Roufaiel MSL, Meyer C. Analytical modeling of hysteretic behavior of R/C frames. *Journal of Structural Engineering* 1987; **113**(3):429–444.
4. Aghagholizadeh M, Massumi A. Relation between dynamic characteristics and damage index of RC-MRFs using non-linear incremental dynamic analyses. *Proceedings of the 15th World Conference on Earthquale Engineering*, Lisbon, Portugal, 2012.
5. Dipasquale E, Ju J-W, Askar A, Cakmak AS. Relation between global damage indices and local stiffness degradation. *Journal of Structural Engineering* 1990; **116**(5):1440–1456.
6. Massumi A, Moshtagh E. A new damage index for RC buildings based on variations of nonlinear fundamental period. *Structural Design of Tall and Special Buildings* 2013; **22**(1):50–61. DOI:10.1002/tal.656.
7. Ou X, He Z, Ou J. Seismic collapse margin of structures using modified mode-based global damage model. Proccedings of the *15th World Conference on Earthquake Engineering*, Lisbon, Portugal, 2012.
8. Williams MS, Sexsmith RG. Seismic damage indices for concrete structures: a state-of-the-art review. *Earthquake Spectra* 1995; **11**(2):319–349.

9. Cordova PP, Deierlein GG, Mehanny SSF, Cornell CA. Development of a two-parameter seismic intensity measure and probabilistic assessment procedure. *Proceedings of the 2nd U.S.–Japan Workshop on Performance-based Earthquake Engineering for Reinforced Concrete Building Structures*, Sapporo, Kokkaido, Japan, 2001.
10. Hutchinson TC, Chai YH, Boulanger RW, Idriss IM. Estimating inelastic displacements for design: extended pile-shaft-supported bridge structures. *Earthquake Spectra* 2004; **20**(4):1081–1094.
11. Kadas K, Yakut A, Kazaz I. Spectral ground motion intensity based on capacity and period elongation. *Journal of Structural Engineering* 2011; **137**(3):401–409. DOI:10.1061/(ASCE).
12. Katsanos EI, Sextos AG, Manolis GD. Selection of earthquake ground motion records: a state-of-the-art review from a structural engineering perspective. *Soil Dynamics and Earthquake Engineering* 2010; **30**(4):157–169. DOI:10.1016/j.soildyn.2009.10.005.
13. CEN. Eurocode 8: Design of structures for earthquake resistance. Part 1: General rules, seismic actions and rules for buildings. Brussels, Belgium, 2003.
14. ASCE 7-10. Minimum design loads for buildings and other structures. *ASCE Standard No. 007-10*. Reston, VA, 2010.
15. FEMA P-750. NEHRP recommended seismic provisions for new buildings and other structures. Washington, DC, 2009.
16. Sextos AG, Katsanos EI, Manolis GD. EC8-based earthquake record selection procedure evaluation: validation study based on observed damage of an irregular R/C building. *Soil Dynamics and Earthquake Engineering* 2011; **31**(4): 583–597. DOI:10.1016/j.soildyn.2010.10.009.
17. Trifunac DM, Ivanovic SS, Todorovska IM. Apparent periods of a building. II: time-frequency analysis. *Journal of Structural Engineering* 2001; **127**(5):527–537.
18. Mucciarelli M, Masi A, Gallipoli MR, Harabaglia P, Vona M, Ponzo F. Analysis of RC building dynamic response and soil-building resonance based on data recorded during a damaging earthquake (Molise, Italy, 2002). *Bulletin of the Seismological Society of America* 2004; **94**(5):1943–1953. DOI:10.1785/012003186.
19. Mucciarelli M, Vona M, Ditommaso R. Experimental measurement of fundamental periods of damaged R/C buildings. *Proceedings of the 15th World Conference on Earthquake Engineering*, Lisbon, Portugal, 2012.
20. Kashima T, Kitagawa Y. Dynamic characteristics of an 8-storey building estimated from strong motion records. *Proceedings of the 1st European Conference on Earthquake Engineering and Seismology*, Geneva, Switzerland, 2006.
21. Clinton JF, Bradford CS, Heaton TH, Favela J. The observed wander of the natural frequencies in a structure. *Bulletin of the Seismologica Society of America* 2006; **96**(1):237–257. DOI:10.1785/0120050052.
22. Masi A, Vona M. Experimental and numerical evaluation of the fundamental period of undamaged and damaged RC framed buildings. *Bulletin of Earthquake Engineering* 2010; **8**(3):643–656. DOI:10.1007/s10518-009-9136-3.
23. Pinho R, Elnashai AS. Dynamic collapse testing of a full-scale four storey rc frame. *ISET Journal of Earthquake Technology* 2000; **37**(4):143–163.
24. Pinto A, Verzeletti G, Molina FJ, Varum R, Pinho R, Coelho E. Pseudo-dynamic tests on non-seismic resisting rc frames (bare and selective retrofit frames). *EUR Report 20244*, ICONS Project, Joint Research Centre - Ispra, Italy, 2002.
25. Jeong S-H, Elnashai AS. Analytical assessment of an irregular rc full scale 3D test structure. *Report for Mid-America Earthquake Center*, Department of Civil and Environmental Engineering, Univeristy of Illinois at Urbana-Champaign, 2004.
26. Negro P, Mola E, Molina FJ, Magonette GE. Full-scale PSD testing of a torsionally unbalanced three-storey non-seismic rc frame. *Proceedigns of the 13th World Conference of Earthquake Engineering*, Vancouver, Canada, 2004.
27. Zembaty Z, Kowalski M, Pospisil S. Dynamic identification of a reinforced concrete frame in progressive states of damage. *Engineering Structures* 2006; **28**(5):668–681. DOI:10.1016/j.engstruct.2005.09.025.
28. Mwafy AM, Elnashai AS. Static pushover versus dynamic collapse analysis of RC buildings. *Engineering Structures* 2001; **23**(5):407–424.
29. Lin L, Naumoski N, Foo S, Saatcioglu M. Elongation of the fundamental periods of reinforced concrete frame buildings during nonlinear seismic response. *Proccedings of the 14th World Conference on Earthquake Engineering*, Beijing, China, 2008.
30. Katsanos EI, Sextos AG, Elnashai AS. Prediction of inelastic response periods of buildings based on intensity measures and analytical model parameters. *Engineering Structures* 2014; **71**:161–177.
31. Calvi G-M, Pinho R, Crowley H. State-of-the-knowledge on the period elongation of RC buildings during strong ground shaking. *Proceedings of the 1st European Conference on Earthquake Engineering and Seismology*, Geneva, Switzerland, 2006.
32. Dunand F, Gueguen P, Bard P-Y, Rodgers J, Celebi M. Comparison of the dynamic parameters extracted from weak, moderate and strong motion recorded in buildings. *Proceedings of the 1st European Conference on Earthquake Engineering and Seismology*, Geneva, Switzerland, 2006.
33. Michel C, Gueguen P. Time – frequency analysis of small frequency in civil engineering structures under weak and strong motions using a reassignment method. *Structural Health Monitoring* 2010; **9**(2):159–171. DOI:10.1177/1475921709352146.
34. Biot MA. Analytical and experimental methods in engineering seismology. *Transactions of the American Society of Civil Engineering* 1943; **108**:365–408.
35. Housner GW, Martel RR, Alford JL. Spectrum analysis of strong-motion earthquakes. *Bulletin of the Seismological Society of America* 1953; **43**(2):97–119.
36. Kappos AJ. Evaluation of behaviour factors on the basis of ductility and overstrength studies. *Engineering Structures* 1999; **21**(9):823–835.

37. Newmark NM, Hall WJ. Earthquake spectra and design. *EERI Monograph*. University of California: Berkeley, 1982.
38. Elghadamsi FE, Mohraz B. Inelastic earthquake spectra. *Earthquake Engineering and Structural Dynamics* 1987; **15**(1):91–104.
39. Krawinkler H, Nassar AA. Seismic design based on ductility and cumulative damage demands and capacities. *Nonlinear Seismic Analysis and Design of Reinforced Concrete Buildings*, Fajfar P, Krawinkler H, (eds). Elsevier Applied Science: New York, 1992.
40. Borzi B, Calvi GM, Elnashai AS, Faccioli E, Bommer JJ. Inelastic spectra for displacement-based seismic design. *Soil Dynamics and Earthquake Engineering* 2001; **21**(1):47–61.
41. Chopra AK, Goel RK. Evaluation of NSP to estimate seismic deformation: SDF systems. *Journal of Structural Engineering* 2000; **126**(4):482–490.
42. Riddell R, Garcia JE, Garces E. Inelastic deformation response of SDOF systems subjected to earthquakes. *Earthquake Engineering and Structural Dynamics* 2002; **31**(3):515–538. DOI:10.1002/eqe.142.
43. Miranda E, Ruiz-García J. Influence of stiffness degradation on strength demands of structures built on soft soil sites. *Engineering Structures* 2002; **24**(10):1271–1281.
44. Chopra AK, Chintanapakdee C. Inelastic deformation ratios for design and evaluation of structures: single-degree-of-freedom bilinear systems. *Journal of Structural Engineering* 2004; **130**(9):1309–1319.
45. Ruiz-García J, Miranda E. Inelastic displacement ratios for evaluation of structures built on soft soil sites. *Earthquake Engineering and Structural Dynamics* 2006; **35**(6):679–694. DOI:10.1002/eqe.552.
46. Mollaioli F, Bruno S. Influence of site effects on inelastic displacement ratios for SDOF and MDOF systems. *Computers and Mathematics with Applications* 2008; **55**(2):184–207. DOI: 10.1016/j.camwa.2007.04.005
47. Eser M, Aydemir C, Ekiz I. Inelastic displacement ratios for structures with foundation flexibility. *KSCE Journal of Civil Engineering* 2012; **16**(1):155–162. DOI:10.1007/s12205-012-1266-5.
48. FEMA-356. Prestandard and commentary for the seismic rehabilitation of buildings. Washington, DC, 2000.
49. FEMA-450. NEHRP recommended provisions for seismic regulations for new buildings and other structures. Washington, DC, 2004.
50. Reinhorn AM, Roh H, Sivaselvan M, Kunnath SK, Valles RE, Madan A, *et al.* IDARC2D version 7.0: a program for the inelastic damage analysis of structures. *Technical Report MCEER-09-0006*, University at Buffalo, State University of New York, 2009.
51. Abdelnaby AE, Elnashai AS. Performance of degrading reinforced concrete frame systems under the Tohoku and Christchurch earthquake sequences. *Journal of Earthquake Engineering* 2014; **18**(7):1009–1036. DOI: 10.1016/j.camwa.2007.04.005
52. Chopra AK. *Dynamics of Structures: Theory and Applications to Earthquake Engineering*. Prentice-Hall: Upper Saddle River, NJ, 2001.
53. Elnashai AS, McGlure DC. Effect of modelling assumptions and input motion characteristics on seismic design parameters of RC bridge piers. *Earthquake Engineering and Structural Dynamics* 1996; **25**(5):435–463.
54. Chiou B, Darragh R, Gregor N, Silva W. NGA project strong-motion database. *Earthquake Spectra* 2008; **24**(1):23–44. DOI:10.1193/1.2894831.
55. Rathje EM, Faraj F, Russell S, Bray JD. Empirical relationships for frequency content parameters of earthquake ground motions. *Earthquake Spectra* 2004; **20**(1):119–144. DOI:10.1193/1.1643356.
56. Mathworks Inc. MATLAB: the language of technical computing, v.R2010a, Natick, Massachusetts, U.S.A., 2010.
57. Ruiz-García J, Miranda E. Inelastic displacement ratios for evaluation of existing structures. *Earthquake Engineering and Structural Dynamics* 2003; **32**(8):1237–1258. DOI:10.1002/eqe.271.
58. Miranda E. Inelastic displacement ratios for structures on firm sites. *Journal of Structural Engineering* 2000; **126**(10):1150–1159.
59. Shome N, Cornell CA, Bazzurro P, Carballo EJ. Earthquakes, records and nonlinear responses. *Earthquake Spectra* 1998; **14**(3):469–500.
60. Baker JW, Cornell CA. A vector-valued ground motion intensity measure consisting of spectral acceleration and epsilon. *Earthquake Engineering and Structural Dynamics* 2005; **34**(10):1193–1217. DOI:10.1002/eqe.474.
61. Bommer JJ, Martínez-Pereira A. The effective duration of earthquake strong motion. *Journal of Earthquake Engineering* 1999; **3**(2):127–172.
62. Trifunac DM, Brady AG. A study on the duration of strong earthquake ground motion. *Bulletin of the Seismological Society of America* 1975; **65**(3):581–626.
63. Husid LR. Caracteristicas de terremotos. *Analisis general. Rev. del IDIEM 8*, Santiago de Chile, 1969.
64. Hancock J, Bommer JJ. Using spectral matched records to explore the influence of strong-motion duration on inelastic structural response. *Soil Dynamics and Earthquake Engineering* 2007; **27**(4):291–299. DOI:10.1016/j.soildyn.2006.09.004.
65. Hancock J, Bommer JJ. A state-of-knowledge review of the influence of strong-motion duration on structural damage. *Earthquake Spectra* 2006; **22**(3):827–845. DOI:10.1193/1.2220576.
66. Chai YH. Incorporating low-cycle fatigue model into duration-dependent inelastic design spectra. *Earthquake Engineering and Structural Dynamics* 2005; **34**(1):83–96. DOI:10.1002/eqe.422.
67. Di Sarno L. Effects of multiple earthquakes on inelastic structural response. *Engineering Structures* 2013; **56**:673–681. DOI: 10.1016/j.engstruct.2013.05.041
68. Goda K, Taylor CA. Effects of aftershocks on peak ductility demand due to strong ground motion records from shallow crustal earthquakes. *Earthquake Engineering and Structural Dynamics* 2012; **41**(15):2311–2330. DOI:10.1002/eqe.2188.

69. Goda K. Nonlinear response potential of mainshock–aftershock sequences from Japanese earthquakes. *Bulletin of the Seismological Society of America* 2012; **102**(5):2139–2156. DOI:10.1785/0120110329.
70. Ruiz-García J, Negrete-Manriquez JC. Evaluation of drift demands in existing steel frames under as-recorded far-field and near-fault mainshock–aftershock seismic sequences. *Engineering Structures* 2011; **33**(2):621–634. DOI: 10.1016/j.engstruct.2010.11.021
71. Araújo M, Macedo L, Castro JM, Delgado R. Influence of code-based record selection methods on the seismic assessment of existing steel buildings. *Proceedings of the 4th International Conference on Computational Methods for Structural Dynamics and Earthquake Engineering*, Kos, Greece, 2013.